# Optical bands of $Cr^{3+}$ induced by $Mg^{2+}$ ions in $LiNbO_3$:Cr,Mg

E. Camarillo,* J. Tocho,† I. Vergara, E. Díeguez, J. García Solé, and F. Jaque
*Universidad Autónoma de Madrid, Departamento de Física Aplicada C-IV, Cantoblanco 28049, Madrid, Spain*
(Received 22 March 1991; revised manuscript received 11 September 1991)

In this paper, the role of Mg ions in the optical properties of $Cr^{3+}$ (absorption, luminescence, and lifetime) in doubly doped $LiNbO_3$ single crystals is analyzed. Additional $R$ lines (denoted as $R_1''$ and $R_2''$), associated with $Cr^{3+}$ ions perturbed by nearby $Mg^{2+}$ ions, were observed. Divalent magnesium ions affect also the $^4T_1$ and $^4T_2$ excited-state levels of $Cr^{3+}$ ions, producing a red shift in the $^4A_2 \rightarrow {}^4T_1$ and $^4A_2 \rightarrow {}^4T_2$ absorption bands. This red shift explains the change observed in the color of Mg-doped samples. The crystal-field parameters and Racah parameters of this $Cr^{3+}$ defect site are reported and compared with those corresponding to singly doped crystals.

## I. INTRODUCTION

There is renewed interest in the study of the optical properties of transition-metal and rare-earth ions in $LiNbO_3$ single crystals because of their potential applications in electro-optic and laser technologies.[1] Unfortunately $LiNbO_3$ is susceptible to optical damage (photorefractive effect) that reduces the applicability of these crystals in nonlinear optical devices.[2] However, in Mg-doped $LiNbO_3$, (more than 5 mol. % of MgO) the optical damage is almost inhibited[3] and stable laser operation has been achieved in $Md^{3+}$-activated samples.[4] Despite this positive result, little is known about the role of Mg ions in the optical properties of $LiNbO_3$ crystals activated with other impurities. The presence of Mg ions could produce changes or alterations in the optical properties of doped $LiNbO_3$ crystals, which may be important for future optical applications. In fact, it has been reported that in $LiNbO_3$:Cr and $LiNbO_3$:Nd the addition of $Mg^{2+}$ leads to the appearance of additional $OH^-$ infrared absorption bands, which have been interpreted as due to the formation of $Cr^3$-$OH^-$-$Mg^{2+}$ and $Nd^{3+}$-$OH^-$-$Mg^{2+}$ centers, respectively.[5,6] Codoping with $Mg^{2+}$ also affects the electron paramagnetic resonance (EPR) and electron-nuclear double resonance (ENDOR) spectra of $Cr^{3+}$ producing modified spectra due to the formation of an additional $Cr^{3+}$ defect site.[7,8] Therefore, the appearance of these additional optical bands of $Cr^{3+}$ in the doubly doped system is also expected. In fact, it was recently shown that codoping $LiNbO_3$:Nd with MgO produces additional fluorescence bands, which can be used to characterize the crystal-field site[9] induced by $Mg^{2+}$ ions ($Li^+$ sites) close to $Nd^{3+}$, located in $Nb^{5+}$ lattice sites, in agreement with previous models.[5–8]

The optical properties of $Cr^{3+}$ ions in different crystals have been much studied.[1] In the case of $LiNbO_3$ crystals, the lowest excited state for $Cr^{3+}$ is the $^4T_2$, from which a broadband emission is observed. However, weak $R$ lines, ascribed to the $^2E \rightarrow {}^4A_2$ transition, can be detected on the high-energy side of the broadband.[10]

Recently, the structure of these fluorescence $R$ lines in $Cr^{3+}$-doped $LiNbO_3$ has been analyzed in detail, and two types of $R$ lines, of $Cr^{3+}$ ions in $Li^+$ and $Nb^{5+}$ sites, were reported.[11]

In this paper, the modification of the optical properties of $Cr^{3+}$:$LiNbO_3$ samples after codoping with 6 mol. % of $Mg^{2+}$ ions is analyzed. The results indicate the formation of these additional fluorescence bands of $Cr^{3+}$ as a consequence of the formation of the additional $Cr^{3+}$ site, which is responsible for the change observed in the color of Mg-codoped $Cr^{3+}$:$LiNbO_3$ samples and explains the color changes previously reported in $LiNbO_3$:Cr,Mg single crystals.[5]

## II. EXPERIMENTAL

The Cr:$LiNbO_3$ and Cr,Mg:$LiNbO_3$ crystals were grown by the Czochralski method from grade I Johnson-Mathey powder in the $c$ direction. The singly doped crystals had a [Cr]/[Nb] concentration ratio of 0.33%, while in doubly doped samples this ratio was 0.15%. The [Mg]/[Nb] concentration ratio was 6%. Samples were cut perpendicular to the $c$ axis (1 mm size), with all their faces polished.

The crystals were colored uniformly, green in singly doped Cr samples and pink in doubly, Cr,Mg-codoped samples.

Emission spectra were excited with an $Ar^+$-ion laser (SP-2020). The emitted light was dispersed in a McPherson (218) monochromator and detected with an EMI-9958-QB photomultiplier tube or Si photodiode connected to a vibrating reed electrometer (Cary 401). Monochromator control and data acquisition were performed using an IBM PS/2 computer.

Absorption spectra were measured with a Cary 17 spectrophotometer. Samples were cooled to low temperature in a closed circle cryorefrigerator with optical access for excitation and detection.

Fluorescence pulses were excited by the second harmonics of a pulsed Nd:YAG laser (532 nm). The data were signal averaged by an oscilloscope (Tektronix 2440) and lifetimes were calculated using least-squares fits.

 

## III. EXPERIMENTAL RESULTS AND DISCUSSION

In order to investigate the effects in the optical properties of $Cr^{3+}$ ions due to the presence of $Mg^{2+}$ ions, two kinds of sample, one singly doped with $Cr^{3+}$ ions and another codoped with $Mg^{2+}$ ions, were used.

Figure 1(a) shows the unpolarized absorption spectrum of $Cr^{3+}$:$LiNbO_3$ crystals at 100 K. According to previously reported data,[10,11] the spectrum consists of two broadbands centered at 480 and 653 nm, with the low-energy band being the more intense. These two broadbands are due to the well-known spin-allowed, $^4A_2 \rightarrow {}^4T_1$ and $^4A_2 \rightarrow {}^4T_2$, vibronic transitions.[10] On the low-energy side of the $^4A_2 \rightarrow {}^4T_2$ broadband, two weak narrow bands located at 723.5 and 725.7 nm can also be observed. Both narrow bands correspond to the so-called $R$ lines, assigned to the $^4A_2 \rightarrow {}^2E$ transition.[10]

The unpolarized absorption spectrum corresponding to doubly, $Cr^{3+}$- and $Mg^{2+}$-codoped $LiNbO_3$ crystals is given in Fig. 1(b). This spectrum also consists of two broadbands, but now centered at 520 and 665 nm. Both bands appear shifted to lower energies relative to the singly doped samples, although this effect is much more pronounced for the high-energy band. Additionally, doubly doped samples show broader vibronic bands than the singly doped samples. These two facts suggest the presence of an additional absorption band for the Cr,Mg:$LiNbO_3$ system. The red shift observed in the high-energy band, together with the weak absorption in the red region, explains the change of color (green to pink) observed between doped and codoped samples. An inspection of Fig. 1(b) reveals also the presence of two very weak narrow bands at about the same position as in the $Cr^{3+}$:$LiNbO_3$ samples.

Regarding the absorption coefficient in both samples, we remark that the observed change cannot be explained by considering only their $Cr^{3+}$-concentration differences, suggesting again the presence of additional absorption transitions.

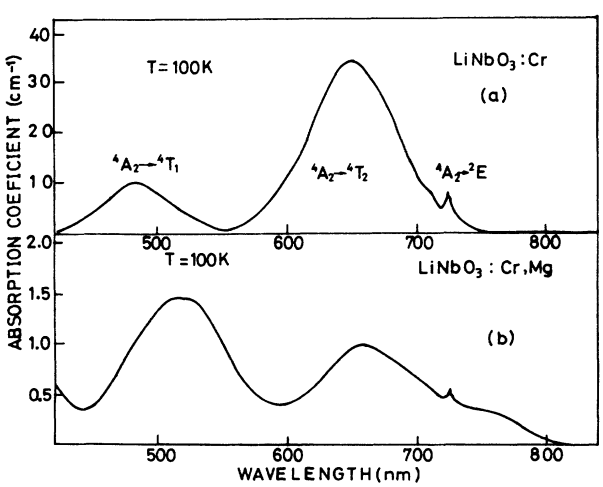


FIG. 1. Unpolarized absorption spectra measured at 100 K. (a) Singly doped $LiNbO^3$:$Cr^{3+}$ samples. (b) Doubly doped $LiNbO_3$Cr,Mg samples.

At this point it is important to mention that a similar change of color was reported to occur in an inhomogeneous $LiNbO_3$:Cr,Mg crystal.[5] Our crystals (singly and doubly doped) were both homogeneously colored and then the color change had to be interpreted as due to the incorporation of magnesium ions. Thus, the crystal field around $Cr^{3+}$ ions is modified and produces additional absorption bands. This idea will be confirmed later by inspection of the fluorescence results.

In order to investigate the creation of additional defect sites in Cr,Mg:$LiNbO_3$ by optical methods, the role of Mg ions in the $^2E \rightarrow {}^4A_2$ and $^4T_2 \rightarrow {}^4A_2$ radiative transitions have been systematically investigated using luminescence techniques.

Figure 2 shows the emission spectra at 20 K in the range from 725 to 745 nm (corresponding to the $R$ lines), for Cr-doped and Cr,Mg-codoped samples exciting with the 488-nm argon line. For Cr:$LibNbO_3$ samples the emission spectrum (continuous line) consists in three narrow bands located at 727.0, 731.3, and 735.7 nm. These narrow emission lines have been previously assigned to the $^2E \rightarrow {}^4A_2$ radiative transition ($R$ lines) from two types of $Cr^{3+}$ centers: $Cr^{3+}$ ions in $Li^+$ or in $Nb^{5+}$ sites.[11]

It is well known that in trigonal symmetry, the $Cr^{3+}$ excited $^2E$ level splits into the $2\bar{A}$ and $\bar{E}$ sublevels[1] and, therefore, two $R$ lines, corresponding to the transitions $\bar{E} \rightarrow {}^4A_2$ ($R_1$ line) and $2\bar{A} \rightarrow {}^4A_2$ ($R_2$ line), should be observed for each $Cr^{3+}$ center. However, at low temperature the low-energy transition is dominant due to a nonradiative relaxation from the upper ($\bar{E}$) to the lower sublevel ($2\bar{A}$).

In Fig. 2, the $R$ lines are denoted following the notation used in Ref. 11. According to this notation, primed lines were tentatively assigned to $Cr^{3+}$ ions entering $Li^+$

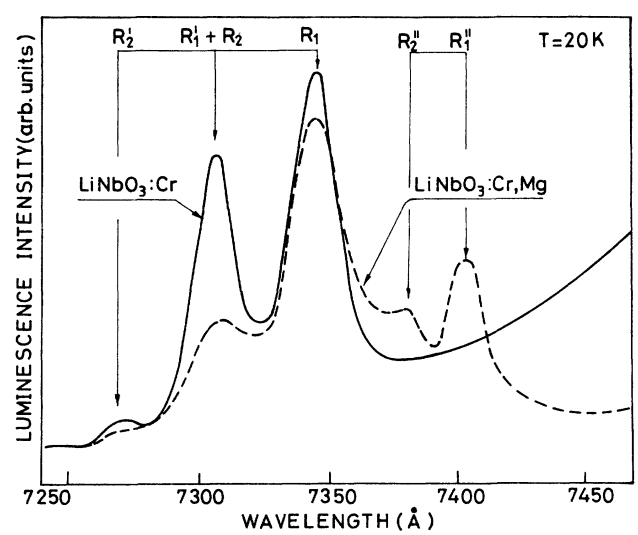


FIG. 2. Unpolarized emission spectra measured at 20 K under $Ar^+$-ion laser excitation at 488 nm. Continuous line corresponds to singly Cr-doped samples and dashed line to doubly, Cr,Mg-codoped samples.

lattice sites and unprimed lines assigned to $Cr^{3+}$ ions entering $Nb^{5+}$ positions. It should be noted that the $R_2$ line is masked by the more intense $R_1'$ line, and therefore only three peaks are observed.

The emission spectrum corresponding to the Cr,Mg-codoped samples excited with the 488-nm argon line is included in Fig. 2 (dashed curve). Notice that two narrow bands located at 739.1 and 741.1 nm appear. In addition, the emission intensities of the $R_2+R_1'$ and $R_2'$ lines clearly decrease. However, these bands will be denoted as $R_1'$ and $R_2''$, respectively. The lifetime of the $R_1$ and $R_1'$ lines was found to be $\sim 400$ $\mu$s, a higher value than that reported in Ref. 11 (276 $\mu$s for the $R_1$ line and 326 $\mu$s for the $R_1'$ line). The lifetime of the $R_1''$ line was found to be $\sim 500$ $\mu$s. The proximity of these bands to the $R$ and $R'$ lines, their narrow structure together with their lifetime value, close to those of the $R$ and $R'$ lines in singly doped samples, indicate that these additional bands are also characteristic of the $^2E \rightarrow {}^4A_2$ transition of $Cr^{3+}$ ions.

As has been commented before, the additional $R_1''$ and $R_2''$ narrow bands appear with a partial extinction of the $R_1'$ and $R_2'$ lines. This fact can be understood by considering the mechanism of formation of the additional Cr,Mg defect center. This mechanism may be the same as that proposed for the Nd-Mg site observed in Nd,Mg:$LiNbO_3$.[9] In this model, $Mg^{2+}$ ions replace some excess percentage of $Li^+$ lattice site[12] ($\simeq 6$ at. %), which in the singly doped sample were occupied by $Nb^{5+}$ sites (and $Cr^{3+}$ sites). These lattice sites are usually called "antisites"[9] but have the same local environment as regular $Li^+$ sites. Therefore, incorporation of $Mg^{2+}$ ions reduces the probability of finding $Cr^{3+}$ ions in $Li^+$ site symmetry so that the intensity of the $R_1'$ and $R_2'$ lines decrease, as observed in Fig. 2.

This result is in good agreement with models previously proposed for these additional $Cr^{3+}$ sites by using infrared absorption[6] or ENDOR and EPR measurements.[7,8] In these models $Cr^{3+}$ ions are replacing $Nb^{5+}$ regular lattice sites and the effect of the proximity of $Mg^{2+}$ ions is to shift the $Cr^{3+}$ ions to a more centered position in their oxygen octahedra.[7] In any case, the changes in the local symmetry have to produce a smaller trigonal splitting between the $2A$ and $E$ levels, resulting in a reduction in the energy separation between the two $R''$ lines, as well as a decrease in the cubic crystal field, which shifts the vibronic absorption bands to lower energies.

Figure 3 shows the emission spectra in the $R$ emission range obtained under different excitation wavelengths of light lying inside the $^4A_2 \rightarrow {}^4T_1$ absorption band. As can be observed, the relative intensities of the $R$ lines are sensitive to the excitation frequency, this variation being more marked for the $R$ lines induced by the Mg ions ($R_1''$ and $R_2''$). It is important to note that the above result was obtained by exciting in the $^4A_2 \rightarrow {}^2E$ transition. Despite this, the result shown in Fig. 3 indicates that selective excitation of the $R$ lines of each site can also be achieved by pumping in the broad vibronic band.

From this result it is clear that the presence of the additional Cr-Mg centers also affects the vibronic bands of $Cr^{3+}$. For confirmation, the broadband emissions associated with the $^4T_2 \rightarrow {}^4A_2$ radiative transition were studied in Cr,Mg:$LiNbO_3$ samples under the same excitation wavelengths used before. As expected, each excitation wavelength produces a different $^4T_2 \rightarrow {}^4A_2$ emission band (see Fig. 4). Excitation at 458 nm produces the same $^4T_2 \rightarrow {}^4A_2$ emission (peaking at 916 nm) observed for the singly, $Cr^{3+}$ doped crystals, while excitation at 514.0 nm leads to a $^4T_2 \rightarrow {}^4A_2$ emission band peaking at 928 nm. Therefore, the presence of $Mg^{2+}$ ions also induces changes in the broad bands associated with the $^4A_2 \rightarrow {}^4T_2$ radiative transitions. Moreover it is clear that the broadening observed in the absorption spectrum of the

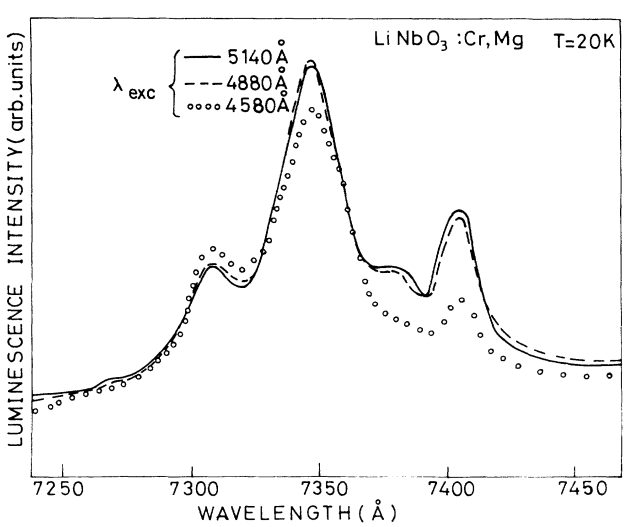


FIG. 3. Emission spectra of doubly doped $LiNbO^3$:Cr,Mg crystals measured at 20 K under different excitation wavelength.

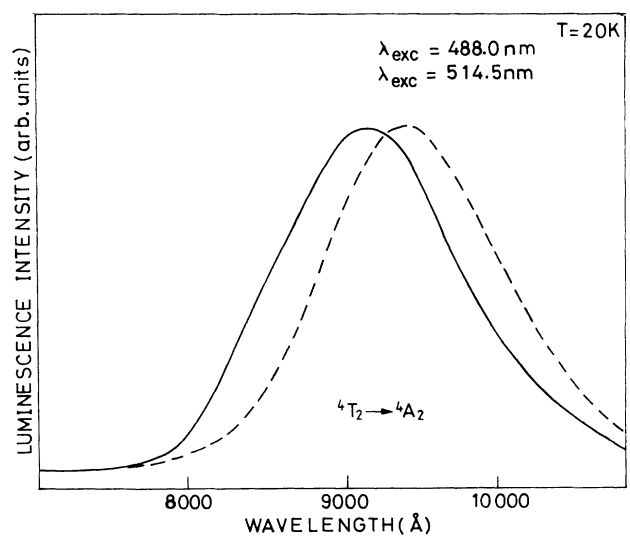


FIG. 4. Emission spectra of $LiNbO_3$:Cr,Mg crystal measured at 20 K under $A^+$-ion laser excitation. Continuous line $\lambda_{exc}=4580$ Å. Dashed line $\lambda_{exc}=5140$ Å.

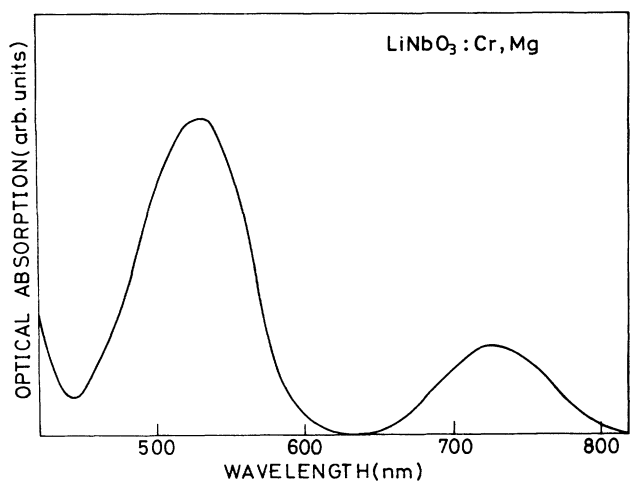


FIG. 5. Convolution of the absorption spectra given in Fig. 1. The curve was obtained normalizing both spectra to the absorption coefficient at 653 nm.

doubly doped samples is due to the appearance vibronic absorption bands of the additional $Cr^{3+}$ crystal-field sites shifted to lower energies. This assignment is at variance with a previous interpretation that assigned these absorption bands to $Cr^{4+}$ ions.[5]

Having taken into account this fact, the optical absorption spectrum shown in Fig. 1(b) has to be considered as due to the convolution of the $Cr^{3+}$ absorption due to $Cr^{3+}$ in $Li^{+}$ and $Nb^{5+}$ sites and $Cr^{3+}$ in $Nb^{5+}$ sites perturbed by nearby $Mg^{2+}$ ions. Figure 5 shows the curve obtained after subtraction of the unperturbed-$Cr^{3+}$-center contribution. This curve was obtained normalizing the two spectra shown in Fig. 1 to the absorption coefficient at 653 nm. The spectrum consists of two broadbands centered at 530 and 730 nm. These bands are assigned to the $^4A_2 \rightarrow {}^4T_1$ and $^4A_2 \rightarrow {}^4T_2$ vibronic transitions of the additional $Cr^{3+}$ defect center. After this assignment we can calculate the cubic crystal-field parameters and the Racah parameters characteristic of the perturbed $Cr^{3+}$ centers. Table I shows these values together with those corresponding to unperturbed $Cr^{3+}$ defect sites (obtained in this work as well as in those previously reported.[10,11] The lifetime values are also given in Table I.

For the Cr:$LiNbO_3$ system, all crystal-field-splitting values $Dq$ are close to 1530 $cm^{-1}$ and only small differences in the Racah $B$ and $C$ parameters are detected. In contrast, the perturbed $Cr^{3+}$ center has a $Dq$ value of 1370 $cm^{-1}$, indicating a lower crystal field (cubic crystal-field approximation) in this case.

Now, considering the experimental data for $Dq$, the ratio between the average chromium to oxygen distances ($R$) for both (perturbed and unperturbed) defect sites can be roughly evaluated using the expression[1]

$$Dq = KR^{-n} ,$$

where $K$ and $n$ are constant for small deviations in $R$. Assuming $n=5$ (point-ion approximation) this ratio is found to be 1.023. This value would indicate a 2.3% distortion in the 6% of lattice defect sites perturbed by $Mg^{2+}$ ions. Thus, an average of 0.13% in the lattice parameter should be expected. This value is not very far from that (0.06%) deduced, with the density change induced by the Mg ions taken into consideration.[13].

Finally, we refer to the radiative lifetimes observed for the $R$ lines. The values observed seem to be shorter than those expected ($\sim$ms) for the $^2E \rightarrow {}^4A_2$ transition, even having taken into account the lowering of cubic symmetry ($C_3$ local symmetry in the unperturbed sites). These short radiative decay times can be explained (in the cubic crystal-field approximation) by considering admixing of $^4T_2$ and $^2E$ levels. Then, the radiative lifetime $\tau$ is given by the expression[10]

$$\frac{1}{\tau} = d^2 \frac{1}{\tau(^4T_2)}$$

with

$$d^2 = \frac{1}{2}\left[1 - \frac{\Delta E}{(4|V_{s.o.}|^2 + \Delta E^2)^{1/2}}\right] ,$$

where $\tau(^4T_2)$ is the lifetime of the $^4T_2 \rightarrow 4A_2$ radiative transition (see Table I), $\Delta E$ the energy separation between $^4T_2$ and $^2E$ levels, and $V_{s.o.}$ the spin-orbit parameter. Using the experimental values obtained in this work and taking 200 $cm^{-1}$ (Ref. 14) for $V_{s.o.}$, the lifetime $\tau$ is found

TABLE I. Values of the crystal-field parameter $Dq$, Racah parameters $B$ and $C$, and lifetime of the singly Cr-doped and doubly, Cr,Mg-codoped $LiNbO_3$ crystals obtained in this work, together with those previously reported.

| Material | $Dq$ ($cm^{-1}$) | $\frac{Dq}{B}$ | $B$ ($cm^{-1}$) | $C$ ($cm^{-1}$) | $\frac{C}{B}$ | $\tau_0(^4T_2 \rightarrow {}^4A_2)$ ($\mu$s) | $\tau_0(^2E \rightarrow {}^4A_2)$ ($\mu$s) |
|---|---|---|---|---|---|---|---|
| $LiNbO_3$:Cr (Ref. 6) | 1530 | 3.17 | 482 | 3150 | 6.53 | 11 | |
| $LiNbO_3$:Cr (Ref. 7) | 1532 | 2.78 | 550 | 2910 | 5.29 | 10.5 | 276($R_1$) 325($R_1'$) |
| $LiNbO_3$:Cr This work | 1532 | 2.76 | 554 | 3224 | 5.82 | 10 | 400($R_1$) 400($R_1'$) |
| $LiNbO_3$:Cr,Mg This work | 1370 | 2.7 | 507 | 3300 | 6.57 | 17 | 500($R_1''$) |

to be $\sim 600$ $\mu$s, which explains the order of magnitude observed. This indicates that mixing of $^2E$ and $^4T_2$ levels takes place in $Cr^{3+}$ for both singly and doubly doped samples, and the $^2E \rightarrow {}^4A_2$ transition becomes partially spin allowed.

## IV. CONCLUSIONS

Absorption and luminescence measurements in Mg-codoped $LiNbO_3$:$Cr^{3+}$ are sensitive to the formation of an additional $Cr^{3+}$ defect site induced by the proximity of Mg ions. This site is considered to be due to $Cr^{3+}$ in the $Nb^{5+}$ site perturbed by a nearby $Mg^{2+}$ ion located in a $Li^+$ site, in agreement with data reported using other techniques.[5–8] The $Dq$ value for the additional $Cr^{3+}$ defect site is smaller than for the unperturbed $Cr^{3+}$ defect sites, indicating a lower cubic crystal field. The red shift detected in the $^4A_2 \rightarrow {}^4T_1$ and $^4A_2 \rightarrow {}^4T_2$ vibronic bands in Mg-codoped samples explains the color change observed in these samples. Finally, the crystal-field parameters, Racah parameters, and lifetime values corresponding to this additional defect center are reported.

## ACKNOWLEDGMENTS

One of us (J. O. Tocho) acknowledges the grant of a sabbatical leave from Ministerio de Educación y Ciencia (Spain), which made this work possible and E. Camarillo wishes to thank the DGADA Universidad Nacional Autónoma de México (UNAM) (Mexico) for financial support. This work has been supported by the Comisión Asesora de Investigación Científica y Técnica (Spain).

*Permanent address: Instituto de Física, Universidad Nacional Autónoma de México, P.O. Box 20-364, 01000 México, Distrito Federal, Mexico.

†Permanent address: Centro de Investigaciones Opticas and Departamento de Física, La Plata, Argentina.

[1]B. Henderson and C. F. Imbush, *Optical Spectroscopy of Inorganic Solids* (Oxford University Press, 1989).

[2]L. F. Johnson and A. A. Ballaman, J. Appl. Phys. **40**, 297 (1969).

[3]G. Zhong, J. Jian, and Z. Wa, *Proceedings of the 11th International Quantum Electronic Conference* (Institute of Electrical and Electronic Engineers, New York, 1980), p. 361.

[4]A. Córdova-Plaza, J. F. Michel, and J. Herbert, IEEE J. Quantum Electron. **QE-23**, 262 (1987).

[5]L. Kovcas, I. Foldvári, I. Cravero, and K. Polgar, Phys. Lett. A **133**, 433 (1988).

[6]L. Kovacs, Zs. Szaller, I. Cravero, I. Foldvári, and C. Zaldo, J. Phys. Chem. Solids. **51**, 417 (1990).

[7]G. Corradi, H. Söthe, J. M. Spaeth, and K. Polgar, J. Phys. Condens. Matter **3**, 1901 (1991).

[8]A. Martín, F. J. Lopez, and F. Agulló-Lopez, J. Phys. Condens. Matter (to be published).

[9]G. Lifante, F. Cussó, J. A. Sanz-García, A. Monteil, B. Varrel, G. Boulon, and J. García Solé, Chem. Phys. Lett. **176**, 482 (1991).

[10]A. M. Glass, J. Chem. Phys. **50**, 1501 (1968).

[11]J. Weiyi, L. Huimin, R. Knutson, and W. M. Yen, Phys. Rev. B **41**, 10 906 (1989).

[12]*Properties of Lithium Niobate* (The Institution of Electrical Engineers, London, 1989), p. 9.

[13]B. C. Grabmair and F. Otto, J. Cryst. Growth **76**, 682 (1986).

[14]M. O. Henry, J. P. Larkin, G. F. Imbusch, *Proceedings of the Royal Irish Academy* (Royal Irish Academy, Dublin, 1975), p. 97.